

Predicting the impact of temperature on metabolic fluxes using resource allocation modelling

Application to polyphosphate accumulating organisms

Páez-Watson, Timothy; van Loosdrecht, Mark C.M.; Wahl, S. Aljoscha

DOI

[10.1016/j.watres.2022.119365](https://doi.org/10.1016/j.watres.2022.119365)

Publication date

2023

Document Version

Final published version

Published in

Water Research

Citation (APA)

Páez-Watson, T., van Loosdrecht, M. C. M., & Wahl, S. A. (2023). Predicting the impact of temperature on metabolic fluxes using resource allocation modelling: Application to polyphosphate accumulating organisms. *Water Research*, 228, Article 119365. <https://doi.org/10.1016/j.watres.2022.119365>

Important note

To cite this publication, please use the final published version (if applicable).
Please check the document version above.

Copyright

Other than for strictly personal use, it is not permitted to download, forward or distribute the text or part of it, without the consent of the author(s) and/or copyright holder(s), unless the work is under an open content license such as Creative Commons.

Takedown policy

Please contact us and provide details if you believe this document breaches copyrights.
We will remove access to the work immediately and investigate your claim.



Predicting the impact of temperature on metabolic fluxes using resource allocation modelling: Application to polyphosphate accumulating organisms

Timothy Páez-Watson^{*}, Mark C.M. van Loosdrecht, S. Aljoscha Wahl¹

Department of Biotechnology, Delft University of Technology, Delft, the Netherlands

ARTICLE INFO

Keywords:

Polyphosphate accumulating organisms
Biosynthesis
Resource allocation
Metabolic modelling
Temperature

ABSTRACT

The understanding of microbial communities and the biological regulation of its members is crucial for implementation of novel technologies using microbial ecology. One poorly understood metabolic principle of microbial communities is resource allocation and biosynthesis. Resource allocation theory in polyphosphate accumulating organisms (PAOs) is limited as a result of their slow imposed growth rate (typical sludge retention times of at least 4 days) and limitations to quantify changes in biomass components over a 6 hours cycle (less than 10% of their growth). As a result, there is no direct evidence supporting that biosynthesis is an exclusive aerobic process in PAOs that alternate continuously between anaerobic and aerobic phases. Here, we apply resource allocation metabolic flux analysis to study the optimal phenotype of PAOs over a temperature range of 4 °C to 20 °C. The model applied in this research allowed to identify optimal metabolic strategies in a core metabolic model with limited constraints based on biological principles. The addition of a constraint limiting biomass synthesis to be an exclusive aerobic process changed the metabolic behaviour and improved the predictability of the model over the studied temperature range by closing the gap between prediction and experimental findings. The results validate the assumption of limited anaerobic biosynthesis in PAOs, specifically “*Candidatus Accumulibacter*” related species. Interestingly, the predicted growth yield was lower, suggesting that there are mechanistic barriers for anaerobic growth not yet understood nor reflected in the current models of PAOs. Moreover, we identified strategies of resource allocation applied by PAOs at different temperatures as a result of the decreased catalytic efficiencies of their biochemical reactions. Understanding resource allocation is paramount in the study of PAOs and their currently unknown complex metabolic regulation, and metabolic modelling based on biological first principles provides a useful tool to develop a mechanistic understanding.

1. Introduction

Biotechnological applications, especially in environmental engineering, strongly depend on the function and stability of microorganisms that interact with each other and with the environment in dynamically changing communities (Konopka, 2009). Further development of tools to study and predict these microbial communities holds the key to improving and expanding the plethora of their applications (Widder et al., 2016). Wastewater treatment is a field of application that, for decades, has relied on the use of microbial communities and modelling to better predict and control the emerging dynamics of such environments (Van Loosdrecht et al., 2015). Extensive experimental

knowledge on these systems has been obtained using long-term lab-scale experiments (Beun et al., 1999; Strous et al., 1998; Lawson et al., 2021; Acevedo et al., 2012). While significant experimental progress was achieved and there is a growing availability of high-throughput data generating techniques (i.e. genomics (Singleton et al., 2021), transcriptomics (Camejo et al., 2019; Oyserman et al., 2016) and proteomics (Kleikamp et al., 2021)), a full characterization and especially mechanistic understanding of these communities remains a challenging task in ecology (Zomorodi and Segrè, 2016). Modelling enables to test different hypothesis of mechanisms and especially whole cell models are crucial to integrate observations, unravel biological principles and predict functions or conditions that are currently inaccessible via

^{*} Corresponding author.

E-mail addresses: T.W.PaezWatson@tudelft.nl, timothypaezw@gmail.com (T. Páez-Watson).

¹ Present address: Lehrstuhl für Bioverfahrenstechnik, Friedrich-Alexander University Erlangen-Nürnberg, Paul-Gordan-Straße 3, 91052 Erlangen, Germany

experimental approaches only (McDaniel et al., 2021).

The enhanced biological phosphorous removal (EBPR) is one of the most studied microbial processes in wastewater treatment and decades of research have unravelled the main biological transformations of this complex engineered ecosystem (Mino et al., 1998; Oehmen et al., 2007; Smolders et al., 1995). In the EBPR system, microorganisms cycle between anaerobic and aerobic phases leading to the enrichment and proliferation of polyphosphate accumulating organisms (PAOs). In this community, one of the most studied bacteria is “*Candidatus Accumulibacter*” (hereafter referred to as *Accumulibacter*) (Oehmen et al., 2007). *Accumulibacter* thrives in a typical EBPR cycle by a complex metabolic strategy involving the cycling of storage polymers: polyphosphate, glycogen and polyhydroxyalkanoates (PHAs) (Smolders et al., 1995).

So far, metabolic modelling approaches for PAOs have been developed and are used with the aim of maintaining stable operations during EBPR processes and/or predicting better conditions favouring simultaneous carbon, phosphorous and nitrogen removal (Van Loosdrecht et al., 2015). Early models such as the ASM3 or TUDP have shown to translate well with process observations, however require extensive recalibration depending on plant properties and environmental conditions. For example, more recent model developments include the effect of putative PAO competitors (Lopez-Vazquez et al., 2009; Oehmen et al., 2010), fermentative PAOs (Varga et al., 2018), storage levels’ effects (Santos et al., 2020), etc. Nevertheless, most current models rely on pre-defined metabolic strategies and consequently reflect the already existing, though not necessarily complete, scientific knowledge on metabolic functions of this ecosystem. Although useful, these features limit the mechanistic understanding of the biological principles governing microbial communities under dynamic conditions.

One of the pre-defined microbial strategy commonly applied in the EBPR models is the assumption of growth being limited to the aerobic phase. Already very early PAO studies suggested that biosynthesis occurs only in the aerobic phase of EBPR systems at expenses of PHA degradation (Comeau et al., 1986; Smolders et al., 1994). Throughout the years, this assumption has been adopted into metabolic models. Interestingly, this assumption has not been verified in-depth besides the observations on the consumption of certain nutrients (e.g. NH_4^+) linked to aerobic growth (Camejo et al., 2019). Many bacterial species that survive under both anaerobic and aerobic conditions grow anaerobically while fermenting substrate (Sawers, 1999; Ribes et al., 2004), hence the validity of this assumption (aerobic biosynthesis) in PAOs is yet to be confirmed.

Due to the slow growth of organisms in EBPR processes, it has been difficult to estimate protein turnover rates and to precisely calculate protein synthesis in different phases of a cycle. A typical EBPR lab-scale setting consist of daily cycles of 6 h with an imposed SRT of 8 days. Thus, theoretically the biomass in the system should renew its proteome in the range of around 32 cycles, meaning that in one cycle the newly produced proteins would account for only 3% of the proteome, and the putative contribution of anaerobic biosynthesis would be even lower. Measuring such small differences in microbial communities is technically challenging considering the inhomogeneity of the culture as well as current limitations such as number of mass spectra acquisition per time (Kleiner, 2019), biased extraction methods to soluble proteins (Sievers, 2018; Helbig et al., 2010), amongst others. Proteomics studies on EBPR sludge from Wilmes et al. (2008) and Wexler et al. (2009) fell short on quantitatively identifying these changes, exemplifying the complications of studying protein synthesis in slow growing systems such as PAOs.

Data from transcriptomic studies, however, seem to indicate a major trend towards aerobic protein biosynthesis. Time series metatranscriptomic data from a highly enriched *Accumulibacter* culture showed different clusters of expression throughout the EBPR cycle (Oyserman et al., 2016). The largest number of transcripts from their study showed trends of transcription during the aerobic phase (identified as aerobic

pattern, redox transition and low phosphate patterns). Although the link from transcription to protein synthesis is not always direct, these results highly suggest that there is a regulation favouring protein synthesis to occur in the aerobic phase. This hypothesis could be further explored experimentally with the use of isotopically labelled acetate fed to a PAOs enrichment, such as the experiments done by (Hesselmann et al., 2000), to identify the fate of ^{13}C anaerobically and aerobically over one or multiple cycles, however up to date such evidence is lacking.

With no final experimental evidence, model based studies considering biosynthesis and resource allocation could be applied to develop an understanding of a putative synthesis of biomass components and furthermore quantify the putative benefit of anaerobic growth. Constraint-based models such as flux balance analysis (FBA) integrating principles from resource allocation represent an opportunity to test a hypothesis regarding biosynthesis during a cyclic, dynamic system (Orth et al., 2010; Rügen et al., 2015). Conditional flux balance analysis (cFBA) is a metabolic modelling tool that was originally developed to predict the metabolism of cyanobacteria under dynamic day/night cycles with strong dependency on resource allocation (Rügen et al., 2015). The characteristics of the cFBA framework and the similarities of these cyclic conditions with those of EBPR make cFBA a suitable method to apply in the context of studying PAOs. Recently, the cFBA method was applied to predict optimal strategies under dynamic environmental conditions encountered during EBPR (Guedes da Silva et al., 2019). Depending on the environmental constraints, different optimal strategies, i.e. organisms accumulating polyphosphate (PAOs), glycogen (GAOs), polyhydroxyalkanoates (PHA-Os) and heterotrophs were predicted. The optimizations resulted in metabolic strategies comparable to those typically observed for *Accumulibacter*. While the general behaviour was correctly predicted, there were quantitative mismatches, suggesting the need for further model development probably beyond parameter calibration. Because the model is strongly shaped by the relation between enzymatic activities and resource allocation, there is potential for expansion in this front.

Enzymatic activities are strongly influenced by temperature and consequently temperature plays a crucial role in shaping the metabolism of microorganisms (Russell, 1990). Implementation of temperature dependencies on metabolic models have shed light on basic biological principles such as a linear relationship between growth rate and ribosome content (Bosdriesz et al., 2015; Metzl-Raz et al., 2017) and optimal proteome allocation as a function of temperature (Mairet et al., 2021). However, these principles result from models for organisms such as *Escherichia coli* at steady-state and may not apply to microbial communities under dynamic conditions. On the other hand, there are extensive experimental studies on the effect of temperature on PAOs metabolism (Brdjanovic et al., 1997, 1998a, 1998b). The current mechanistic understanding of PAOs metabolism with relation to temperatures could be combined with metabolic models such as cFBA to identify metabolic principles governing growth and resource allocation. Especially, at low temperatures, the efficient use of available resources like enzyme capacity are assumed to be crucial for evolutionary competitiveness.

In the current study, we combined the cFBA modelling framework with temperature dependency for PAOs to identify metabolic principles regarding resource allocation. We compared the complete model with and without a constraint on anaerobic biomass synthesis. Our results further validate the assumption on biomass being limited to the aerobic sector of EBPR and shed light on previously unexplored putative regulation on protein biosynthesis.

2. Materials and methods

2.1. Model description

For modelling the metabolism and energy allocation of PAOs, a constrained-based approach named conditional flux balance analysis (cFBA) was used (Rügen et al., 2015). The model and parameters for

PAOs was obtained from [Guedes da Silva et al. \(2019\)](#).

The model consists of 29 metabolites connected by 36 reactions represented in a stoichiometric matrix S . All network reactions and stoichiometry are detailed in Table S1. Different to conventional approaches, only a subset of metabolites (7 metabolites) are considered in steady state by the relation:

$$\bar{S} \cdot v_t = 0,$$

where \bar{S} denotes the stoichiometric matrix subset of steady state metabolites and v_t denotes the fluxes of each reaction at time interval t . The remaining 22 metabolites are dynamic, i.e. are allowed to accumulate or deplete over time (polymers, enzymes and biomass precursors) and their molar amount is updated at each time point by the following relation:

$$M_t = \tilde{S} \cdot v_t + M_{t-1}$$

M_t is a vector that indicates the molar amount of the non-steady state metabolites at time interval t , and \tilde{S} denotes the stoichiometric matrix subset of the dynamic metabolites (not in steady state).

2.1.1. Biomass growth and composition

Growth of the system at the end of the simulation is described as the overall fold-change (α) of the initial metabolite composition (M_0):

$$M_{end} = \alpha * M_0$$

This relation introduces the possibility to simulate a system in a cycle, as the proportions of non-steady state metabolites need to be maintained only at the end of the simulation. The values of M_0 are an outcome of the simulation in order to achieve maximal growth but limited to the total sum of 1 gram dry weight (g_{DW}) by the relation:

$$w^T \cdot M_0 = 1,$$

where w^T is a transposed vector containing the weights that different components have on 1 g_{DW} of biomass. The values in w^T were defined by [Guedes da Silva et al. \(2019\)](#) for glycogen, polyphosphate and PHA levels based on data published by [Acevedo et al. \(2012\)](#). Data published by [Acevedo et al. \(2012\)](#) belong to a reactor performing > 99% phosphate removal with a defined population of > 85% PAOs and show clearly identified cycling of polyphosphate, glycogen, PHB and PHV. Protein content was based on the work of [Yücesoy et al. \(2012\)](#).

2.1.2. Quota definition of compounds

The metabolites that are not in steady state consist of storage polymers (glycogen, polyphosphate, PHB and PH2MV), catalytic metabolites (enzymes and ribosomes) and non-catalytic metabolites (named here as biomass precursors and other proteins). Because some of these metabolites do not reinforce the autocatalytic behaviour of the system, their values in the vector M_0 will tend to be 0 as this vector is an outcome of the simulation to optimize growth. To enforce the synthesis of these compounds, [Rüger et al. \(2015\)](#) introduced the concept of quota compounds following the relation:

$$B_{quotat} M_t \geq C_{quotat} (w^T \cdot M_t)$$

In this relation, B_{quotat} is a matrix containing the index positions in the M vector of the metabolites for which the quota is being defined at time point t . C_{quotat} is a vector containing the values for the said quotas. The indicated relation was used to define minimal quota levels at time 0 for glycogen, polyphosphate and PHAs based on data published by [Acevedo et al. \(2012\)](#). It was also used to define an all-time minimal level of biomass precursors and non-catalytic proteins.

For this research, the concept of quota compounds was slightly modified to include specific and maximum quota compounds at indicated time points.

$$B_{quota_eqt} M_t = C_{quota_eqt} (w^T \cdot M_t)$$

$$B_{quota_maxt} M_t \leq C_{quota_maxt} (w^T \cdot M_t)$$

These additional concepts were used to define a set initial amount of substrate (acetate) at time 0 hours and to enforce its uptake by setting a maximum quota of 0 at 0.5 h of the cycle.

2.1.3. Catalytic and non-catalytic constraints on fluxes

Comparable to conventional FBA, each reaction can be limited according to pre-assigned values in a lower (lb) and upper bound (ub) vector at each time point.

$$lb_t \leq v_t \leq ub_t$$

The lower and upper bounds were used to specify environmental limits on reactions (e.g. during the anaerobic period, oxygen consuming had an ub of 0 mmol/ g_{DW} /h). Otherwise, the upper bounds were defined by the amount of a specific catalyst and the turnover rate of this catalyst ($k_{cat,E}$ values) by:

$$v_t \leq M_{t,E} \cdot k_{cat,E}$$

where $M_{t,E}$ denotes a subsection of M_t containing the molar amount of enzymes at time t and $k_{cat,E}$ a vector with the catalytic turnover number ($k_{cat,E}$) of each enzyme. All reactions from the system except for CO_2 diffusion are catalysed by enzymes or ribosomes. The $k_{cat,E}$ values for each reaction were adapted from the work from [Rüger et al. \(2015\)](#) and if not considered in their research it was obtained from the BRENDA database ([Schomburg et al., 2012](#)). The molar cost of all the enzymes was the assumed to be the same based on the work from [Rüger et al. \(2015\)](#).

2.1.4. Maintenance requirements

Metabolic models commonly consider the expenditure of energy (ATP) for basic maintenance purposes. Here, a constant flux of 0.3980 mmol ATP/ g_{DW} /h was used, based on literature values for PAOs ([Smolders et al., 1995](#)). This value is assumed for the anaerobic as well as aerobic phase, and is independent of the amount of available substrate.

2.1.5. Simulation of dynamic conditions

Simulations were performed considering a typical EBPR cycle: an anaerobic phase of 1.5 h followed by an aerobic phase of 3.5 h. The anaerobic conditions were simulated by setting the upper bound for the electron transport chain (ETC) reaction to 0 mmol O_2 / g_{DW} /h. Conversely, during the aerobic phase the upper bound of this reaction was only limited by the capacity of the respective enzyme constraint. The substrate (acetate) was available at the beginning of the anaerobic phase ($t=0h$) by setting an initial metabolite quota for the starting amount. To enforce rapid consumption, a maximum quota of 0 mmol/ g_{DW} /h was set at 30 min.

2.1.6. Optimization target and algorithm used

The previously defined constraints (equalities and inequalities of the model) are discretized in defined time intervals throughout the cycle. Linear programming was then used to identify possible flux distributions at each time interval without an optimization objective. Thus, the obtained flux distribution for each time point is not an optimal unique solution, but rather a possible solution that fulfils the equality and inequality constraints mentioned so far (steady state metabolites, initial metabolite composition, quotas and enzyme capacities).

The possible solutions can be further constrained for any given α value (fold change of the system). The overall optimal target (maximum possible α value) was set following the approach introduced by [Rüger et al. \(2015\)](#) and used by [Reimers et al. \(2017\)](#) and [Guedes da Silva et al. \(2019\)](#). Briefly, a search for α values that fulfil the linear constraints is performed using an algorithm of binary search until the highest achievable α value is found with a defined accuracy (minimal step-size)

of 10^{-7} . Due to the presence of internal cycles in the metabolic model, the solution obtained is not unique. To further limit the solution space, we identified and limited internal cycles from the available solutions with no effect on the outcome of the simulation.

2.1.7. Temperature dependencies

Temperature was implemented as a parameter affecting the turnover rates (k_{cat}) of individual reactions following the simplified Arrhenius equation from 4 to 20 °C. This relation has been used previously to describe temperature effect on the kinetics of PAOs using a black-box kinetic model (Brdjanovic et al., 1998a; Lopez-Vazquez et al., 2009) and is expressed as:

$$k_{cat}(T) = k_{cat(20)} * \theta^{(T-20^{\circ}C)}$$

where $k_{cat}(T)$ represents the k_{cat} value at temperature T , $k_{cat}(20)$ the k_{cat} value at 20 °C (defined as optimal temperature for PAOs) and theta (θ) the temperature coefficient for the specific reaction in question. The values for θ are reaction specific, and were adapted from the previously determined θ values found in Lopez-Vazquez et al. (2009) and summarized in Table S2. The values for θ of reactions that have not been determined were set within the range of estimated θ values for comparable bioconversions. The effect of the set θ values on the model prediction was evaluated with a general parameter sweep.

2.1.8. Simulation with and without biomass synthesis constrains

To evaluate the effect that biomass growth during the entire cycle or only during the aerobic phase, two simulations were performed. These simulations are referred to as the *unconstrained growth* (no constrains on biosynthesis) and the *aerobic growth* (biosynthesis can only occur during the aerobic period) models. The only difference between both models lays on the upper bounds allowed for the reactions involved in protein and ribosomes production (including enzymes) and synthesis of biomass precursors (BMP) synthesis (See Table S1 for information on the stoichiometry of these reactions). In the *unconstrained growth* model, these

bounds were constrained like all other reactions (set by the catalytic limitations), whereas in the *aerobic growth* model, these upper bounds were set to 0 mmol/g_{dw}/h during the anaerobic phase.

2.2. Software and model availability

All simulations were performed in MATLAB version 9.4 (R2019b) using LINPROG as the linear optimization solver. The original cFBA model was retrieved from Rügen et al. (2015) and the PAOs specific model retrieved from Guedes da Silva et al. (2019). The adapted model used in this study is available at GitLab project ID 39202430 (https://gitlab.com/delft_paos/cFBA_temperature).

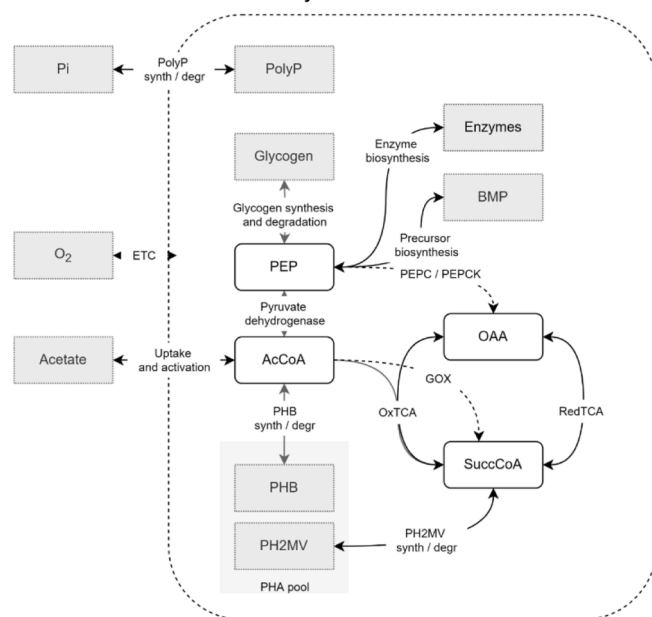
3. Results

3.1. Reference simulation: EBPR cycle with unconstrained growth at 20 °C

We first investigated the predicted metabolic response of the model with *unconstrained growth* (Fig. 1A) in a typical EBPR system at 20 °C and used it as the reference simulation for further comparisons. A total cycle length of 5 h was applied: 1.5 h anaerobic and 3.5 h aerobic. Acetate was enforced to be consumed within 30 min of the anaerobic period to simulate the competition for substrate and obtain the competitive strategy of organisms enriched under this regime (Guedes da Silva et al., 2019). The minimal initial amounts (quota) of storage polymers (polyphosphate, glycogen and PHA) per biomass (mol / g_{dw}) were introduced in the model based on data published by Acevedo et al. (2012). Using these conditions, the reference metabolic response of PAOs simulated was obtained and compared to the experimental profiles from Acevedo et al. (2012) (Fig. 1B).

The simulation reproduced complete acetate consumption and accumulation as PHA (Fig. 1B), while polyphosphate was degraded to provide the required ATP for the uptake and activation of acetate and anaerobic maintenance. Reducing equivalents (modelled as NADH) for

A: Metabolic model used in this study



B: Metabolic profiles predicted by the model with unconstrained growth

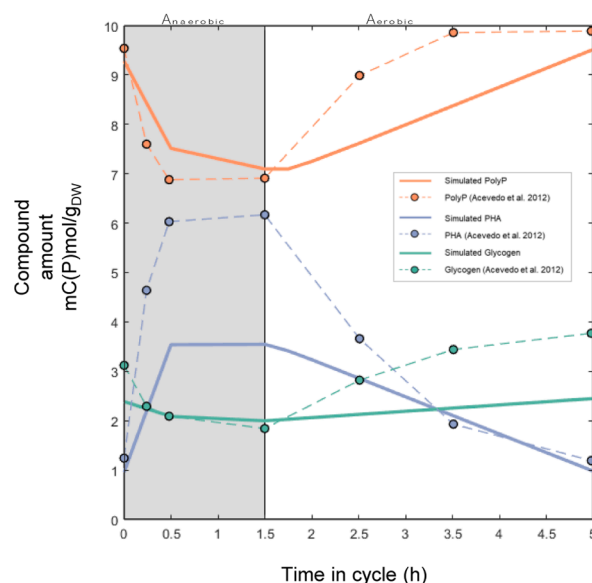


Fig. 1. A) Schematic representation of the reaction network used for the cFBA simulations. Compounds enclosed by grey boxes are dynamic compounds, that can accumulate resp. decrease over time. All other compounds were assumed to reach quasi steady-state. Each reaction is catalyzed by a specific enzyme available at a calculated, dynamic concentration. B) Solid lines: predicted metabolite concentrations of PAOs during an EBPR cycle at 20 °C with unconstrained growth (Guedes da Silva et al., 2019). Circles and dotted lines: experimental data from an EBPR system retrieved from Acevedo et al. (2012). Abbreviations: Inorganic phosphate (Pi), polyphosphate (PolyP), poly-hydroxy-butyrate (PHB), poly-hydroxy-2-methylvalerate (PH2MV), oxaloacetate (OAA), succinyl CoA (SuccCoA), acetyl CoA (AcCoA), phosphoenolpyruvate (PEP), glycogen (Glyc), biomass precursors (BMP), phosphoenolpyruvate carboxylase (PEPC), phosphoenolpyruvate carboxykinase (PEPCCK), glyoxylate shunt (GOX), oxidative and reductive tricarboxylic acid cycle (OxTCA and redTCA respectively), electron transport chain (ETC).

PHA accumulation were provided by glycogen degradation and a fraction of acetate being channelled through the TCA cycle. When oxygen became available (aerobic phase, with activated ETC), the intracellular PHAs were degraded and the resources from this degradation were used to restore the glycogen and polyphosphate pool. Such metabolic strategy observed in the cycling of polymers is typical of *Accumulibacter* (Oehmen et al., 2007; Acevedo et al., 2012; Smolders et al., 1995).

Although the model with *unconstrained growth* predicted typical profiles for *Accumulibacter*, there are some quantitative mismatches with the compared experimental data set (Fig. 1B), mainly regarding the amount of glycogen and PHA used/accumulated within a cycle. This mismatch between prediction and experimental data results in part from a higher contribution of the NADH generated in the TCA cycle leading to lower required flux through glycolysis (Fig. 3, explored in the following subsections). We additionally identified that biosynthesis was active anaerobically in this simulation (mainly synthesising enzymes). To evaluate if the observed mismatches were specific to the chosen condition (EBPR at 20 °C) or based on a systematic feature of our modelling approach, we explored a broad range of different temperatures.

3.2. Simulations for different temperatures

Reported, experimentally determined values of temperature coefficients (θ) in PAOs range from 1.03 for polyphosphate synthesis to up to 1.13 for PHA degradation (See Table S2 and Fig. S1). For other reactions of the metabolic model (TCA cycle, ETC, protein biosynthesis, ribosome synthesis, etc.) no specific θ values for PAOs were found in literature. Therefore, these were assumed to be the same for all uncharacterized reactions and we analysed the impact of this value varying within a range of the previous reported values.

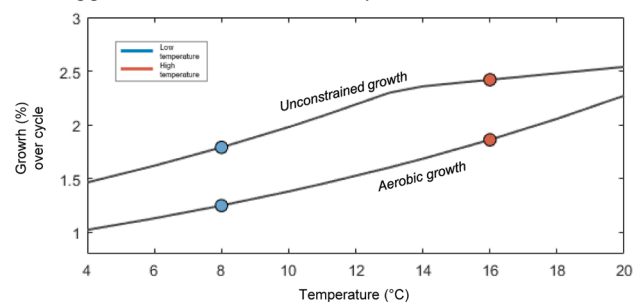
A typical EBPR cycle was simulated ranging between 4 °C and 20 °C. For all simulations, a shift in the metabolic strategy towards lower temperatures was observed (Fig. S2). The tested θ value of uncharacterized reactions did not affect the metabolic shift, but affected the temperature at which the shift was observed (Fig. S2). For example, the simulations indicated a metabolic shift of the system towards colder temperatures below either 13 °C or 18 °C when assuming θ values for uncharacterized reactions with $\theta=1.05$ or 1.15 respectively. From here on, a value of 1.05 was used for the reactions where no experimental value was available.

3.3. Influence of the growth constraint on simulations

With temperature dependencies implemented in the metabolic model, we simulated a typical EBPR cycle of PAOs over a temperature range from 4 °C to 20 °C with no constraints on growth. The results show a decrease in growth yield with a decrease in temperature following two different exponential regions (Fig. 2A: *Unconstrained growth*). In these simulations, the model employed slightly a different metabolic strategy towards lower temperatures resulting in a larger use of glycogen and polyphosphate over the cycle (Fig. 2B: *Unconstrained growth*). We observed that in the studied temperature range, resources were destined for growth in both the anaerobic and aerobic phases. Interestingly, the lower the temperature, the higher contribution anaerobic growth had on the system, especially destined towards enzyme synthesis reactions (reaching up to 25% of all biosynthesis at temperatures below 10 °C).

Although there is no conclusive proof that growth is an exclusive aerobic process in PAOs, we analysed the impact of constraining growth to the aerobic phase only. Particularly, a constraint was introduced to block biosynthesis reactions during anaerobic conditions. The model with these new constraints was used to simulate the previous conditions (typical EBPR cycle of PAOs over a temperature range from 4 °C to 20 °C). The resulting growth yields were lower than those of the *unconstrained growth* model, and similarly decreased towards lower temperatures (Fig. 2A: *aerobic growth* model). This decrease, however, followed a distinct exponential Arrhenius-like curve. Additionally, these

A: Resulting growth of simulations at different temperatures



B: Polymer profiles of the model at high and low temperatures with/without constraints on growth

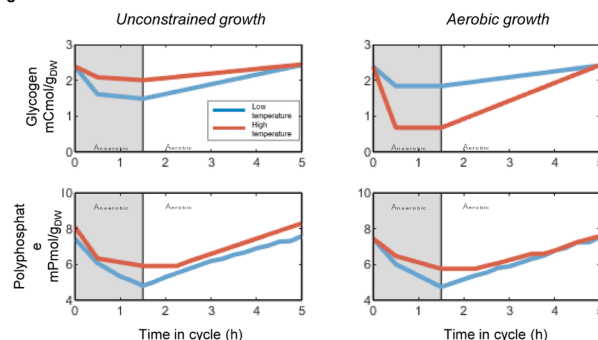


Fig. 2. Predicted biomass yields and intracellular storage pools during an EBPR cycle at different temperatures. (A) Biomass increase at the end of a cycle. A decrease in temperature results in a decrease of biomass synthesis during the cycle of both the unconstrained growth and the aerobic growth model. The red and blue dots indicate simulations that are displayed w.r.t. glycogen and polyphosphate profiles over time (B). (B) Glycogen and polyphosphate over time in an EBPR cycle at 8 °C (blue line) and 16 °C (red line). Left panel represents the profile for the unconstrained growth model and the right panel represents the profiles of the aerobic growth model. For a representation of polymer changes over the entire temperature range, see Fig. S3.

simulations resulted in higher levels of glycogen use at 20 °C than the model with no growth constraints (>3 fold higher) better replicating the results from Acevedo et al. (2012). Towards lower temperatures, less glycogen and more polyphosphate was used in these simulations (Fig. 2B: *Aerobic growth*).

3.4. Comparison and analysis of resource allocation strategies

The different predictions obtained over the studied temperature range are compared in terms of their resource allocation. Especially, we focus on the allocation of electrons (in form of NADH) and energy (in the form of ATP) by analysing reactions using or generating these metabolites. For this, we analysed the generation and consumption of NADH (Fig. 3) and ATP (Fig. 4) during the anaerobic phase of each simulation with respect to the amount of acetate consumed. Note that the metabolism of PAOs is strongly constrained in the anaerobic phase, hence we primarily focus on the anaerobic phase of each simulation.

The model with no constraints on anaerobic growth predicted that, anaerobically, NADH and ATP were allocated towards biosynthesis of enzymes, and this allocation grew larger at lower temperatures (Figs. 3 and 4: *unconstrained growth* model). The increased need for these resources for biosynthesis was met with an increased flux of glycogen degradation (up to 280% more turnover) supplying both the required ATP and NADH in this model, which fits the observations of a larger turnover of glycogen towards lower temperatures (Fig. 2: *Unconstrained growth*).

Predictions of the model allowing only aerobic growth indicated an opposite trend than that of the unconstrained model. Namely, the

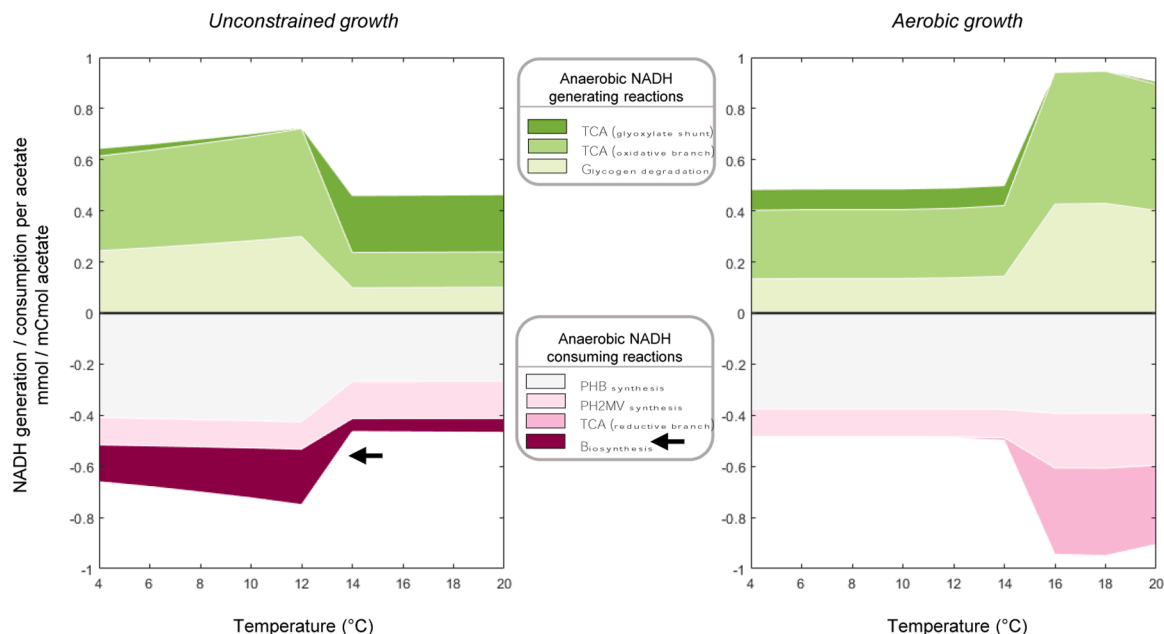


Fig. 3. Balance and reactions involved in the NADH generation (green) and consumption (magenta) during the anaerobic phase of the unconstrained growth (left panel) model and the aerobic growth (right panel) model. Black arrow indicates the use of NADH for biosynthetic reactions showcasing the main difference in the structure between both models. Biosynthesis comprised all reactions synthesizing enzymes, ribosomes and biomass precursors. For the specific reaction stoichiometry, please see Table S1. Abbreviations: tricarboxylic acid cycle (TCA), poly-hydroxy-butyrate (PHB), poly-hydroxy-2-methylvalerate (PH2MV).

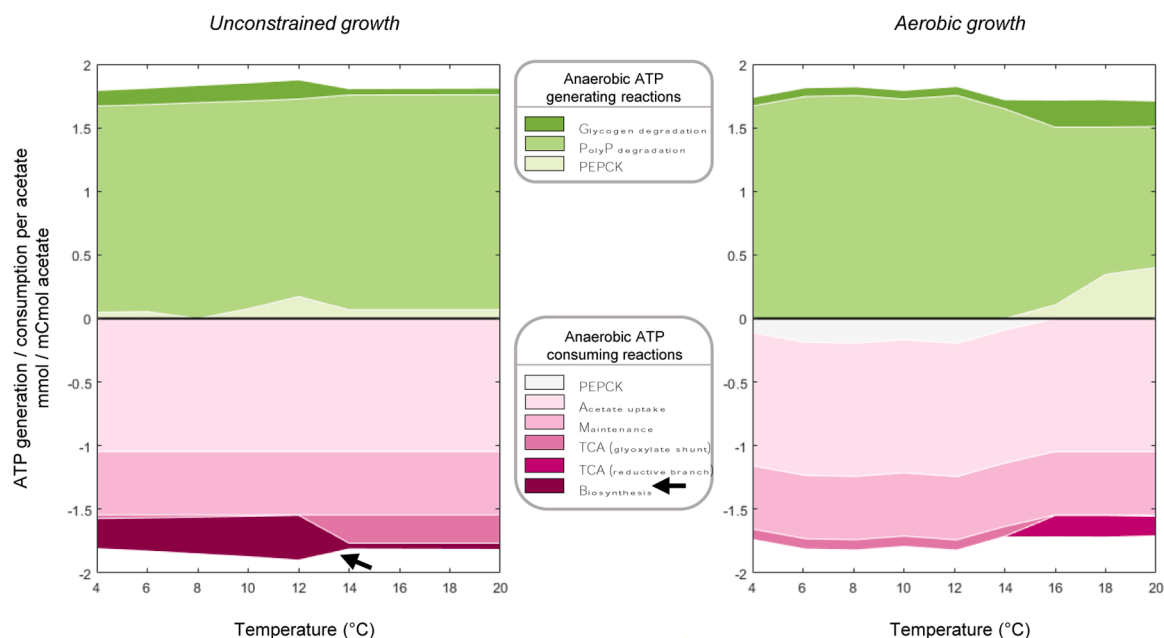


Fig. 4. Balance and reactions involved in the ATP generation (green) and consumption (magenta) during the anaerobic phase of the PAOs simulations at different temperatures of the unconstrained growth (left panel) model and the aerobic growth (right panel) model. Black arrow indicates the use of ATP for biosynthetic reactions showcasing the main difference in the structure between both models. Biosynthesis comprised all reactions synthesizing enzymes, ribosomes and biomass precursors. For the specific reaction stoichiometry, please see Table S1. Abbreviations: polyphosphate (PolyP), phosphoenolpyruvate carboxykinase (PEPCK), tricarboxylic acid cycle (TCA).

turnover of NADH was larger at higher temperatures (Fig. 3) resulting in a larger turnover of glycogen as described in the previous section (Fig. 2). Interestingly, the larger amounts of glycogen degraded at higher temperatures led to an overproduction of electrons than required only for acetate uptake, leading to a higher accumulation of PH2MV as a sink of these electrons. Additionally, the source of ATP produced anaerobically in this model shifted from a nearly full contribution of

polyphosphate at lower temperatures towards a shared contribution of polyphosphate degradation, glycogen degradation and PEPCK at higher temperatures (Fig. 4: Aerobic growth model). Note that PEPCK is a reversible reaction, and as such acts as both an ATP sink and source at lower and higher temperatures respectively.

4. Discussion

4.1. The model with only aerobic growth predicts better polymer use of PAOs

The metabolic shift predicted by the *unconstrained growth* model indicated that at lower temperatures larger amounts of glycogen were being degraded than at higher temperatures (Fig. 2B: *unconstrained growth*). This result was surprising and opposite to what has been observed experimentally and described in literature. Brdjanovic et al. (1997) exposed PAOs enrichments at short term temperature changes and observed that at lower temperatures less glycogen was used overall, contradictory with the predictions of this model. Further, Brdjanovic et al. (1998a) confirmed the same experimental observations in PAOs enrichments on longer term temperature effects. This same behaviour has been reproduced by using kinetic models (Lopez-Vazquez et al., 2009; Garcia-Usach et al., 2006) and even proven to hold true for Glycogen Accumulating Organisms (GAOs) under similar conditions (Lopez-Vazquez et al., 2008).

On the other hand, the constraint limiting biosynthesis to be an exclusive aerobic process resulted in predictions more in line with the described literature over the studied temperature range (Brdjanovic et al., 1998a; Brdjanovic et al., 1997; Lopez-Vazquez et al., 2009; Whang and Park, 2006). I.e. the amount of glycogen used anaerobically in a cycle increased with an increase in temperature (Figs. 2, 3 and 4: *aerobic growth*). Further, the overall amount of glycogen used (and consequently PHA accumulated) at 20 °C was also larger than in the *unconstrained growth* model, resulting in improved model predictions when compared to the experimental dataset obtained by Acevedo et al. (2012) (Fig. 1). Not only the predictions of the *aerobic growth* model approximated better the results from Acevedo et al. (2012), but also the anaerobic stoichiometric yields for glycogen, PHA and polyphosphate fit better within the observed yields from multiple PAOs enrichments at 20 °C (summarized in Welles et al. (2015)) (Fig. 5) further supporting the validity of the added biological constraint of this model.

Other than the direct effect observed on polymer cycling, the model

also improved in fulfilling a basic principle of systems biology: linear relationship between growth rate and ribosome content (Fig. S4). Such a biological principle is paramount for biological systems at balanced growth (Bosdriesz et al., 2015; Metzl-Raz et al., 2017), and should not be an exception for PAOs. The simulations with no growth constraints at different temperatures showed no such linear relation (Fig. S4 A & B). However, once the constraint on limiting anaerobic biosynthesis was introduced, a linear relation between growth rate and ribosome content emerged (Fig. S4 C & D). We note that recently Mair et al. (2021) showed that at higher temperatures, this linear relationship breaks, nevertheless the temperature range of this study is below such threshold.

The different predictions from both models arose as a consequence of resource limitation in a system that was tightly constrained by its catalytic capacities (Rügen et al., 2015). At lower temperatures, the decrease in catalytic efficiency of each metabolic process resulted in lower flux capacities that could only be resolved by either producing larger enzymatic levels or adopting a different metabolic strategy. Such limitations in energy metabolism are known to strongly shape the proteome and metabolic strategy of microorganisms (Chen and Nielsen, 2019). This was clearly observed in the *unconstrained growth* model, when at lower temperatures there was an increased flux of biosynthesis during the anaerobic phase (Figs. 3 and 4) in order to maintain metabolic fluxes high. These higher fluxes also resulted in higher growth yields of the unconstrained growth model as compared to the growth constrained model. Such biosynthetic fluxes were balanced with increased glycogen degradation that generated the required NADH, ATP and metabolic precursors. As these results strongly contradict what has been observed experimentally, we conclude that indeed anaerobic biosynthesis is severely limited in PAOs.

The aforementioned discussed results highlight the validity of the newly introduced constraint as a general biological principle that could apply to PAOs such as *Accumulibacter*, but might even be generalized to organisms that are adapted to live under dynamic anaerobic/aerobic environments such as those encountered in EBPR or estuary sediments. Next, we attempt to give a biological meaning to the introduced constraint on limiting biomass synthesis and hypothesise on the possible regulation behind it.

4.2. Putative regulation of biosynthesis under dynamic conditions

Biomass synthesis in PAOs has been commonly assumed to be limited to only the aerobic phase (Comeau et al., 1986; Smolders et al., 1994). However, these assumptions have never been proven experimentally. Since anaerobic growth is very common among bacteria it cannot simply be assumed as non-existing in PAOs.

We suggest that the limit on anaerobic biosynthesis is likely caused due to a dynamics shift in the energetic and redox state over an EBPR cycle. The presence of an external electron acceptor (i.e. oxygen) has been proven to strongly affect the redox state of cells (Sun et al., 2012). That is, anaerobically the NADH/NAD⁺ ratio increases, limiting reactions that are near equilibrium in the cell. Although not studied in depth during EBPR we hypothesise that this ratio is dynamically changing over a cycle (Zhao et al. (2021) showed direct measurements of this ratio, although this methodology has not been extensively proven). Similarly, we hypothesise that polyphosphate degradation could be initiated anaerobically by thermodynamic control caused by a shift in the ATP/AMP balance in the cell (hypothesised in early PAOs research by Comeau et al. (1986)) as a combined consequence of fast acetate uptake and the changed redox state. However, the synthesis and polymerization of proteins requires a relatively low ATP/AMP ratio, being opposite to that required for polyphosphate degradation (Urry, 2011), making both physiological processes to be thermodynamically opposed. More research is required in the dynamics of the redox and energetic state of PAOs to further understand physiological mechanisms of organisms living under EBPR like conditions.

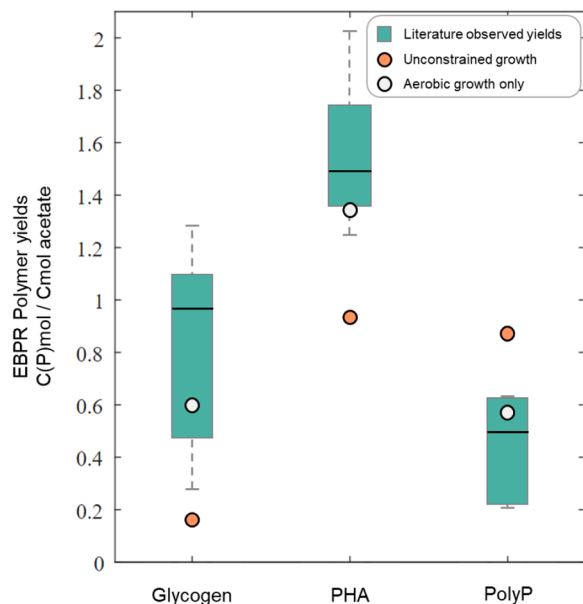


Fig. 5. Anaerobic yields of Glycogen (Cmol glycogen / Cmol acetate), PHA (Cmol PHA / Cmol acetate) and polyphosphate (Pmol / Cmol acetate) on acetate over a typical EBPR cycle at 20 °C. The figure indicates a (green) box plot summarizing typical literature values for PAOs enrichments from several research groups (summarized in Welles et al. (2015)), and the predictions at 20 °C from the (orange) unconstrained growth model and (light grey) aerobic growth model.

4.3. First principles modelling approach to predict PAOs metabolism

The dynamic resource allocation modelling approach applied resulted in typical polymeric profiles that PAOs exhibit in a EBPR cycle (Fig. 1) without the need of parameter calibration or predefinition of metabolic strategies. Thus, the employed method could be used not only to understand the environmental selection on PAOs, GAOs and PHA-AOs as was done by Guedes da Silva et al. (2019), but to test basic metabolic principles shaping optimality in dynamic conditions. This modelling approach represents an alternative to traditional used modelling approaches that rely on experimental yields and kinetics (Van Loosdrecht et al., 2015; Lopez-Vazquez et al., 2009; Oehmen et al., 2010; Varga et al., 2018; Santos et al., 2020), but is however not intended to be used as an indicator of EBPR process control or performance.

The applied model in this research could be used as a tool to expand our current understanding of redox and energetic state of bacterial cells under dynamic conditions. For example, here we identified a potential shift in the sources of NADH and ATP (Figs. 3 and 4 respectively) as a function of temperature. Further studying these individual contributions, this model could explain the reason behind the large variation in P/C ratio obtained by different research groups when studying PAOs enrichments (summarized in da Silva et al. (2020)). This model is not intended to be used for monitoring waste water treatment plants, but rather to gather fundamental knowledge that could help improve our mechanistic understanding of organisms commonly encountered in said processes.

5. Conclusions

From this research, we can conclude that:

- Resource allocation theory delivers a strong framework to analyse metabolic processes in microbial communities typically found in wastewater treatment systems.
- Integrating temperature into a FBA models of organisms living in dynamic conditions allows for deeper understanding of resource allocation limitations of cells.
- Based on the resource allocation theory results, the biosynthetic routes of Accumulibacter are limited to the aerobic phase of the EBPR cycle.

Contributors

TPW and AW conceived the research. TPW performed simulations and analysed results. TPW, MvL and AW wrote the manuscript.

Declaration of Competing Interest

The authors declare that they have no known competing financial interests or personal relationships that could have appeared to influence the work reported in this paper.

Data availability

I have shared a link to the data and code of the publication in the manuscript.

Acknowledgments

This work was supported by SIAM Gravitation Grant 024.002.00, the Netherlands Organization for Scientific Research (NWO).

Supplementary materials

Supplementary material associated with this article can be found, in

the online version, at doi:10.1016/j.watres.2022.119365.

References

- Acevedo, B., Oehmen, A., Carvalho, G., Seco, A., Borrás, L., Barat, R., 2012. Metabolic shift of polyphosphate-accumulating organisms with different levels of polyphosphate storage. *Water Res.* 46, 1889–1900.
- Beun, J.J., Hendriks, A., Van Loosdrecht, MCM, Morgenroth, E., Wilderer, P.A., Heijnen, J.J., 1999. Aerobic granulation in a sequencing batch reactor. *Water Res.* 33, 2283–2290.
- Bosdriesz, E., Molenaar, D., Teusink, B., Bruggeman, F.J., 2015. How fast-growing bacteria robustly tune their ribosome concentration to approximate growth-rate maximization. *FEBS J.* 282, 2029–2044.
- Brdjanovic, D., Loosdrecht, MCMV, Hooijmans, C.M., Alaerts, G.J., Heijnen, J.J., 1997. Temperature effects on physiology of biological phosphorus removal. *J. Environ. Eng.* 123, 144–153.
- Brdjanovic, D., Logemann, S., Loosdrecht, MCMV, Hooijmans, C.M., Alaerts, G.J., Heijnen, J.J., 1998a. Influence of temperature on biological phosphorus removal: process and molecular ecological studies. *Water Res.* 32, 1035–1048.
- Brdjanovic, D., Loosdrecht, MCMV, Hooijmans, C.M., Alaerts, G.J., Heijnen, J.J., 1998b. Minimal aerobic sludge retention time in biological phosphorus removal systems. *J. Biotechnol. Bioeng.* 60, 326–332.
- Camejo, P.Y., Oyserman, B.O., McMahon, K.D., Noguera, D.R., 2019. 'Integrated omic analyses provide evidence that a "Candidatus Accumulibacter phosphatis" strain performs denitrification under microaerobic conditions'. *Msystems* 4 (1), e00193-18.
- Chen, Y., Nielsen, J., 2019. Energy metabolism controls phenotypes by protein efficiency and allocation. *Proc. Natl. Acad. Sci.* 116, 17592–17597.
- Comeau, Y., Hall, K.J., Hancock, R.W., Oldham, W.K., 1986. Biochemical model for enhanced biological phosphorus removal. *Water Res.* 20, 1511–1521.
- Garcia-Usach, F., Ferrer, J., Bouzas, A., Seco, A., 2006. Calibration and simulation of ASM2d at different temperatures in a phosphorus removal pilot plant. *Water Sci. Technol.* 53, 199–206.
- Guedes da Silva, L., Tomás-Martínez, S., Loosdrecht, MCMV, Aljoscha Wahl, S., 2019. The environment selects: modeling energy allocation in microbial communities under dynamic environments. *bioRxiv*, 689174.
- Helbig, A.O., Heck, A.J.R., Slijper, M., 2010. Exploring the membrane proteome—challenges and analytical strategies'. *J. Proteom.* 73, 868–878.
- Hesselmann, R.P., Von Rummel, R., Resnick, S.M., Hany, R., Zehnder, A.J.B., 2000. Anaerobic metabolism of bacteria performing enhanced biological phosphate removal. *Water Res.* 34, 3487–3494.
- Kleikamp, H.B., Pronk, M., Tugui, C., Silva, L.G.d.a., Abbas, B., Lin, Y.M., Loosdrecht, MCMV, Pabst, M., 2021. Database-independent de novo metaproteomics of complex microbial communities. *Cell Syst.* 12, 375–383 e5.
- Kleiner, M., 2019. 'Metaproteomics: much more than measuring gene expression in microbial communities'. *Msystems* 4, e00115–e00119.
- Konopka, A., 2009. What is microbial community ecology? *ISME J.* 3, 1223–1230.
- Lawson, C.E., Nuijten, G.H., Graaf, R.M. de, Jacobson, T.B., Pabst, M., Stevenson, D., Jetten, M.S.M., Noguera, D.R., McMahon, K.D., Amador-Noguez, D., 2021. Autotrophic and mixotrophic metabolism of an anammox bacterium revealed by in vivo 13C and 2H metabolic network mapping. *ISME J.* 15, 673–687.
- Lopez-Vazquez, C.M., Song, Y.-I., Hooijmans, C.M., Brdjanovic, D., Moussa, M.S., Gijzen, H.J., Loosdrecht, MCMV, 2008. Temperature effects on the aerobic metabolism of glycogen-accumulating organisms. *Biotechnol. Bioeng.* 101, 295–306.
- Lopez-Vazquez, C.M., Oehmen, A., Hooijmans, C.M., Brdjanovic, D., Gijzen, H.J., Yuan, Z., Loosdrecht, MCMV, 2009. 'Modeling the PAO-GAO competition: effects of carbon source, pH and temperature'. *Water Res.* 43, 450–462.
- Mairet, F., Gouzé, J.-L., Jong, H.de, 2021. Optimal proteome allocation and the temperature dependence of microbial growth laws. *NPJ Syst. Biol. Appl.* 7, 1–11.
- McDaniel, E.A., Wahl, S.A., Ishii, S., Pinto, A., Ziels, R., Nielsen, P.H., McMahon, K.D., Williams, R.B.H., 2021. Prospects for multi-omics in the microbial ecology of water engineering. *Water Res.* 205, 117608.
- Metzl-Raz, E., Kafri, M., Yaakov, G., Soifer, I., Gurvich, Y., Barkai, N., 2017. Principles of cellular resource allocation revealed by condition-dependent proteome profiling. *Elife* 6, e28034.
- Mino, T.MCM, Van Loosdrecht, MCM, Heijnen, J.J., 1998. Microbiology and biochemistry of the enhanced biological phosphate removal process. *Water Res.* 32, 3193–3207.
- Oehmen, A., Lemos, P.C., Carvalho, G., Yuan, Z., Keller, J., Blackall, L.L., Reis, M.A.M., 2007. Advances in enhanced biological phosphorus removal: from micro to macro scale. *Water Res.* 41, 2271–2300.
- Oehmen, A., Carvalho, G., Lopez-Vazquez, C.M., Van Loosdrecht, MCM, Reis, M.A.M., 2010. Incorporating microbial ecology into the metabolic modelling of polyphosphate accumulating organisms and glycogen accumulating organisms. *Water Res.* 44, 4992–5004.
- Orth, J.D., Thiele, I., Palsson, B.O., 2010. What is flux balance analysis? *Nat. Biotechnol.* 28, 245–248.
- Oyserman, B.O., Noguera, D.R., Rio, T.G.d., Tringe, S.G., McMahon, K.D., 2016. Metatranscriptomic insights on gene expression and regulatory controls in Candidatus Accumulibacter phosphatis. *ISME J.* 10, 810–822.
- Rügen, M., Bockmayr, A., Steuer, R., 2015. Elucidating temporal resource allocation and diurnal dynamics in phototrophic metabolism using conditional FBA. *Sci. Rep.* 5, 15247.
- Reimers, A.-M., Knoop, H., Bockmayr, A., Steuer, R., 2017. Cellular trade-offs and optimal resource allocation during cyanobacterial diurnal growth. *Proc. Natl. Acad. Sci.* 114, E6457–E6465.

- Ribes, J., Keesman, K., Spanjers, H., 2004. Modelling anaerobic biomass growth kinetics with a substrate threshold concentration. *Water Res.* 38, 4502–4510.
- Russell, N.J., 1990. Cold adaptation of microorganisms. *Philos. Trans. R. Soc. Lond. B* 326, 595–611.
- Santos, JMM, Rieger, L., Lanham, A.B., Carvalheira, M., Reis, MAM, Oehmen, A., 2020. A novel metabolic-ASM model for full-scale biological nutrient removal systems. *Water Res.* 171, 115373.
- Sawers, G., 1999. 'The aerobic/anaerobic interface'. *Curr. Opin. Microbiol.* 2, 181–187.
- Schomburg, I., Chang, A., Placzek, S., Söhlgen, C., Rother, M., Lang, M., Munaretto, C., Ulas, S., Stelzer, M., Grote, A., 2012. BRENDA in 2013: integrated reactions, kinetic data, enzyme function data, improved disease classification: new options and contents in BRENDA. *Nucleic Acids Res.* 41, D764–DD72.
- Sievers, S., 2018. Membrane proteomics in Gram-positive bacteria: two complementary approaches to target the hydrophobic species of proteins. *Microb. Proteom.* 1841, 21–33.
- Silva, da, Guedes, L., Gamez, K.O., Gomes, J.C., Akkermans, K., Welles, L., Abbas, B., Loosdrecht, MCMV, Wahl, S.A., 2020. 'Revealing the metabolic flexibility of "candidatus accumulibacter phosphatis" through redox cofactor analysis and metabolic network modeling'. *Appl. Environ. Microbiol.* 86 (24), e00808-20.
- Singleton, C.M., Petriglieri, F., Kristensen, J.M., Kirkegaard, R.H., Michaelsen, T.Y., Andersen, M.H., Kondrotaitė, Z., Karst, S.M., Dueholm, M.S., Nielsen, P.H., 2021. Connecting structure to function with the recovery of over 1000 high-quality metagenome-assembled genomes from activated sludge using long-read sequencing. *Nat. Commun.* 12, 1–13.
- Smolders, GJF, Van der Meij, J, Van Loosdrecht, MCM, Heijnen, JJ, 1994. Model of the anaerobic metabolism of the biological phosphorus removal process: stoichiometry and pH influence. *Biotechnol. Bioeng.* 43, 461–470.
- Smolders, GJF, Van der Meij, J, Van Loosdrecht, MCM, Heijnen, JJ, 1995. A structured metabolic model for anaerobic and aerobic stoichiometry and kinetics of the biological phosphorus removal process. *Biotechnol. Bioeng.* 47, 277–287.
- Strous, M., Heijnen, J.J., Gijs Kuenen, J., Jetten, MSM, 1998. The sequencing batch reactor as a powerful tool for the study of slowly growing anaerobic ammonium-oxidizing microorganisms. *Appl. Microbiol. Biotechnol.* 50, 589–596.
- Sun, F., Dai, C., Xie, J., Hu, X., 2012. Biochemical issues in estimation of cytosolic free NAD/NADH ratio. *PLoS One* 7, e34525.
- Urry, D.W., 2011. Thermodynamics of protein structure formation and function. Application of Thermodynamics to Biological and Materials Science. (IntechOpen).
- Van Loosdrecht, MCM, Lopez-Vazquez, CM, Meijer, SCF, Hooijmans, CM, Brdjanovic, D, 2015. Twenty-five years of ASM1: past, present and future of wastewater treatment modelling. *J. Hydroinform.* 17, 697–718.
- Varga, E., Hauduc, H., Barnard, J., Dunlap, P., Jimenez, J., Menniti, A., Schauer, P., Vazquez, C.M.L., Gu, A.Z., Sperandio, M., 2018. Recent advances in bio-P modelling—a new approach verified by full-scale observations'. *Water Sci. Technol.* 78, 2119–2130.
- Welles, L., Tian, WD, Saad, S, Abbas, B, Lopez-Vazquez, CM, Hooijmans, CM, Van Loosdrecht, MCM, Brdjanovic, D, 2015. Accumulibacter clades Type I and II performing kinetically different glycogen-accumulating organisms metabolisms for anaerobic substrate uptake. *Water Res.* 83, 354–366.
- Wexler, M., Richardson, D.J., Bond, P.L., 2009. Radiolabelled proteomics to determine differential functioning of Accumulibacter during the anaerobic and aerobic phases of a bioreactor operating for enhanced biological phosphorus removal. *Environ. Microbiol.* 11, 3029–3044.
- Whang, L.-M., Park, J.K., 2006. Competition between polyphosphate-and glycogen-accumulating organisms in enhanced-biological-phosphorus-removal systems: effect of temperature and sludge age. *Water Environ. Res.* 78, 4–11.
- Widder, S., Allen, R.J., Pfeiffer, T., Curtis, T.P., Wiuf, C., Sloan, W.T., Cordero, O.X., Brown, S.P., Momeni, B., Shou, W., 2016. Challenges in microbial ecology: building predictive understanding of community function and dynamics. *ISME J.* 10, 2557–2568.
- Wilmes, P., Andersson, A.F., Lefsrud, M.G., Wexler, M., Shah, M., Zhang, B., Hettich, R.L., Bond, P.L., VerBerkmoes, N.C., Banfield, J.F., 2008. Community proteogenomics highlights microbial strain-variant protein expression within activated sludge performing enhanced biological phosphorus removal. *ISME J.* 2, 853–864.
- Yücesoy, E., Lüdemann, N., Lucas, H., Tan, J., Denecke, M., 2012. Protein analysis as a measure of active biomass in activated sludge. *Water Sci. Technol.* 65, 1483–1489.
- Zhao, J., Xie, S., Luo, Y., Li, X., 2021. NADH accumulation during DPAO denitrification in a simultaneous nitrification, denitrification and phosphorus removal system. *Environ. Sci. Water Res. Technol.* 7, 1819–1827.
- Zomorodi, A.R., Segrè, D., 2016. Synthetic ecology of microbes: mathematical models and applications. *J. Mol. Biol.* 428, 837–861.